

# When Less is More: The LLM Scaling Paradox in Context Compression

Ruishan Guo<sup>1,2,\*</sup> Yibing Liu<sup>1,\*</sup> Guoxin Ma<sup>1,3</sup> Yan Wang<sup>1</sup> Yueyang Zhang<sup>1</sup> Long Xia<sup>1</sup> Kecheng Chen<sup>4</sup>  
 Zhiyuan Sun<sup>1</sup> Daiting Shi<sup>1</sup>

## Abstract

Scaling up model parameters has long been a prevalent training paradigm driven by the assumption that larger models yield superior generation capabilities. However, under lossy context compression in a compressor–decoder setup, we observe a *Size-Fidelity Paradox*: increasing the compressor size can lessen the faithfulness of reconstructed contexts though training loss decreases. Through extensive experiments across models from 0.6B to 90B, we coin this paradox arising from two dominant factors: 1) *knowledge overwriting*: larger models increasingly replace source facts with their own prior beliefs, *e.g.*, “the white strawberry” → “the red strawberry”; and 2) *semantic drift*: larger models tend to paraphrase or restructure content instead of reproducing it verbatim, *e.g.*, “Alice hit Bob” → “Bob hit Alice”. By holding model size fixed, we reflect on the emergent properties of compressed context representations. We show that the culprit is not parameter count itself, but the excessive semantic capacity and amplified generative uncertainty that accompany scaling. Specifically, the increased rank of context embeddings facilitates prior knowledge intrusion, whereas higher entropy over token prediction distributions promotes rewriting. Our results complement existing evaluations over context compression paradigm, underpinning a breakdown in scaling laws for faithful preservation in open-ended generation.

## 1. Introduction

The scaling hypothesis is dominating the training principle of large language models (Kaplan et al., 2020; Hoffmann et al., 2022; Lai et al., 2025; Sengupta et al., 2025). It posits that increasing the number of model parameters leads

<sup>\*</sup>Equal Contribution. <sup>1</sup>Baidu Inc., Beijing, China. <sup>2</sup>Shenzhen International Graduate School, Tsinghua University. <sup>3</sup>Xi'an Jiaotong University. <sup>4</sup>City University of Hong Kong.

Preprint. February 11, 2026.

to enhanced performance, which has been corroborated across a variety of model families (*e.g.*, GPT (Achiam et al., 2023), LLaMA (Grattafiori et al., 2024), and Qwen (Yang et al., 2025a)) and applications (*e.g.*, computer vision (Minderer et al., 2023; Yang et al., 2025b), recommendation system (Zhang et al., 2024; Cai et al., 2025), code generation (Yang et al., 2025b)). However, in this paper, we identify a *Size-Fidelity Paradox* in context compression: beyond a certain parameter scale, larger models underperform smaller ones in preserving source fidelity.

Language models in context compression mostly act as compressors which map natural language tokens into a small set of memory tokens (Ge et al., 2023; Li et al., 2025b;a), thus facilitating downstream decoding. In line with the prevalence of scaling hypothesis, existing studies also report that larger compressors improve compression quality across various tasks (Dai et al., 2025; Lin et al., 2025). Yet, as illustrated in Fig. 1, a side-fidelity paradox exists. That is, when reconstructing the phrase *blue-banded bee and the bee shakes pollen loose from flowers*, lite compressor (*e.g.*, Qwen-3 0.6B) produces minor literal deviations that preserve the original meaning. In contrast, larger compressors (*e.g.*, LLaMA-3.2 90B) exhibit two critical failure modes: 1) *knowledge overwriting*, where source facts (*blue-banded bee*) are replaced with the model’s internal knowledge, *i.e.*, *honey bee*, and 2) *semantic drift*, where reconstructions deviate from the literal source content, *i.e.*, *the flower vibrates its anthers to shake pollen loose onto bees*.

While somewhat dissatisfying, standard metrics on reconstruction performance fail to capture this degradation (Longpre et al., 2021; Ming et al., 2024; Long et al., 2025). To this end, this paper designs two diagnostic QA tasks that isolate knowledge overwriting and semantic drift. We conduct extensive experiments across two mainstream LLM families, Qwen and LLaMA, spanning 0.6B to 90B parameters at multiple compression ratios. The results systematically confirms both the existence and generality of the paradox. Beyond verification, these tasks further establish a principled evaluation framework that reveals fidelity failures invisible to surface metrics.

To further answer how scaling-induced changes in model architecture cause larger compressors to sacrifice literal ac-

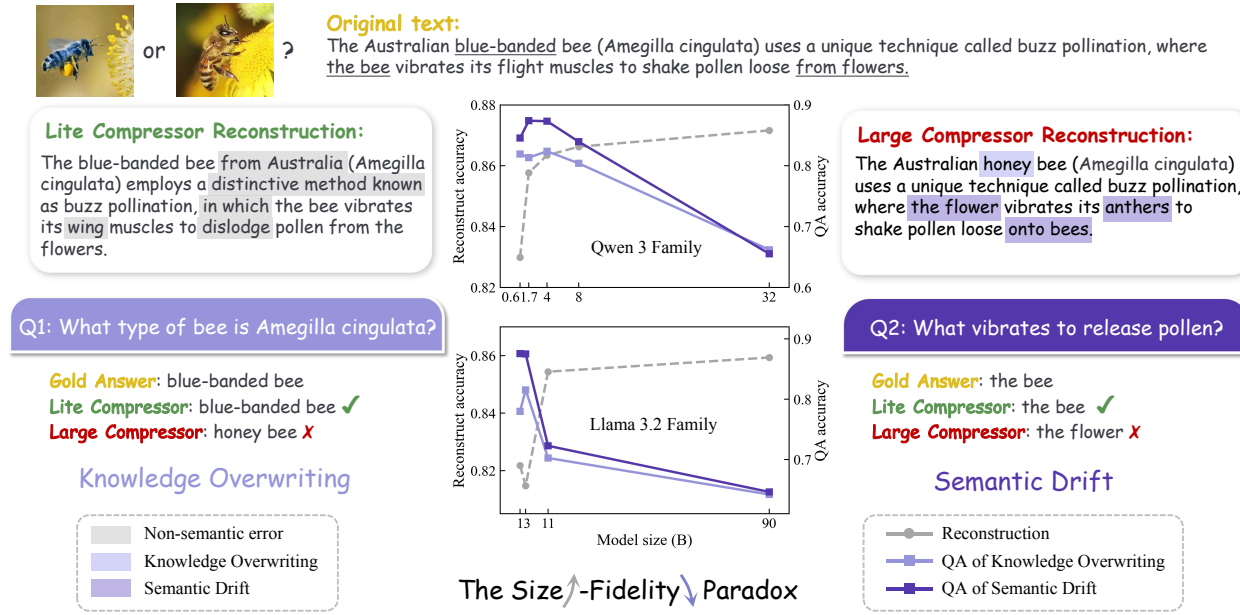


**Figure 1. The Size-Fidelity Paradox in context compression. (Left & Right)** A qualitative case study illustrating the breakdown of faithfulness. While the Lite compressor preserves factual details (Q1, Q2), the Large compressor succumbs to two distinct failure modes: (1) *knowledge overwriting*, where source facts are replaced by priors (e.g., hallucinating “honey bee” instead of “blue-banded bee”); and (2) *semantic drift*, where the causal relationship is distorted (e.g., “bee pollinates flower” → “flower pollinates bee”). **(Center)** Quantitative analysis across Qwen and Llama families confirms this paradox is systematic. As model size scales up (*x*-axis), surface-level *Reconstruction* scores (dashed lines) remain high, yet *QA accuracy* (solid lines) significantly degrades. This divergence indicates that larger compressors prioritize their own semantic capacity and priors over the faithful preservation of the source context.

curacy, we probe the internal properties of compressor models via targeted probes and mechanistic analysis. We find that model size is a surface-level factor; the deeper causes lie in two core capabilities: *semantic capacity* and *generative uncertainty*. Specifically, larger models exhibit higher effective rank, dispersing representations across broader semantic subspaces where parametric knowledge can more easily interfere. Similarly, they also exhibit lower conditional entropy, reflecting confident generative priors that readily override ambiguous encodings. Our mechanistic analysis reveals a fundamental tradeoff: the very properties that enable complex reasoning in large models interfere with the rigid fidelity required for faithful reconstruction.

In sum up, our contributions are as follows:

- We identify a LLM scaling paradox in context compression: larger compressor models can underperform smaller ones though construction performance improves, contradicting prevailing assumptions.
- We present two diagnostic tasks to uncover the underlying performance in context compression regarding knowledge overwriting and semantic drifting problems. This complements current limitations of existing compression evaluation, providing a more robust assessment framework.

- We uncover the mechanistic drivers of this paradox, showing how semantic capacity and generative uncertainty trade off with fidelity preservation.

## 2. Related Work

### 2.1. Scaling Laws in Language Models

Scaling laws have become a central principle in modern language modeling. Extensive work (Kaplan et al., 2020; Hoffmann et al., 2022; Ruan et al., 2024; Team et al., 2025) shows that increasing model scale generally reduces training loss and improves performance across many generation and reasoning tasks (Wang et al., 2024; Yang et al., 2025b; Cai et al., 2025), and larger models often exhibit stronger world knowledge and emergent abilities. However, recent studies have increasingly indicated that scaling does not guarantee uniformly better behavior. In particular, some work (Wei et al., 2023; Zhou et al., 2024; Chen et al., 2025) reports that larger models can be less reliable on challenging inputs, for example by producing errors with higher confidence or exhibiting weaker calibration. While these findings highlight important limitations of scaling, they primarily examine answer correctness and reliability in question answering or reasoning. These studies therefore provide limited insight into how scaling behaves in tasks where faithful reproduc-

tion of the input is required. Our work addresses this gap by studying scaling behavior in a fidelity-critical compressor–decoder setting, where the objective is to reconstruct the source text with minimal distortion rather than to generate a plausible paraphrase. Notably, while larger compressors can achieve better reconstruction metrics, smaller models perform better on fidelity-oriented downstream evaluation, revealing a size–fidelity paradox. Beyond identifying this phenomenon, we further analyze why scaling leads to such degradation and explain the mechanisms by which properties amplified by scale can undermine literal reconstruction.

## 2.2. Evaluation of Long-Context Compression

Long-context compression has been widely studied to reduce the cost of long-context modeling and to make long inputs usable under limited context windows (Li et al., 2023; Yen et al., 2024; Li et al., 2025c; Berton et al., 2025). Most approaches (Ge et al., 2023; Li et al., 2025a; Dai et al., 2025) follow a compressor–decoder paradigm, where a long sequence is encoded into a compact latent representation and a decoder reconstructs text conditioned on it. Correspondingly, prior work (Ge et al., 2023; Dai et al., 2025) largely evaluates these methods through reconstruction-centric protocols, comparing performance across compression ratios and model scales using standard metrics (e.g., training loss, perplexity, and  $n$ -gram overlap scores such as BLEU (Papineni et al., 2002) and ROUGE (Lin, 2004)).

While convenient, such metrics can be superficial and incomplete proxies for compression quality. They primarily reward fluency and surface similarity, but do not distinguish information genuinely recovered from the compressed representation from plausible content supplied by a model’s parametric priors. As a result, a model can obtain high reconstruction scores while still changing or losing important details from the original text. Motivated by this limitation, we propose a usage-oriented evaluation perspective that assesses compression by its functional support for realistic downstream tasks, providing a more faithful measure of what the compressed representation actually preserves.

## 3. Preliminaries

**Compressor-Decoder Architecture.** The prevalent training paradigms in context compression (Ge et al., 2023; Dai et al., 2025; Li et al., 2025a) employs compressor-decoder setup, where one language model acts as a compressor transforming the discrete input sequence into a set of continuous latent embeddings (memory tokens); whereas, another language model performs as the decoder, targeting at reconstructing compressed representation to original text.

Formally, let  $\mathcal{V}$  denote a vocabulary of tokens. Given an input sequence  $\mathbf{x} = (x_1, \dots, x_L) \in \mathcal{V}^L$ , the objective of

context compression is to learn a compressor  $f_\theta$ , which maps the input  $\mathbf{x}$  to a latent tensor  $\mathbf{Z} \in \mathbb{R}^{M \times d}$ :

$$\mathbf{Z} = f_\theta(\mathbf{x}), \quad \text{where } M \ll L. \quad (1)$$

Here,  $d$  represents the hidden dimension, and  $M$  is the number of memory slots. The compression rate is defined as  $\rho = L/M$ . The decoder  $g_\phi$  operates as a causal language model conditioned on  $\mathbf{Z}$ . It estimates the probability distribution of the original sequence:

$$P_\phi(\mathbf{x}|\mathbf{Z}) = \prod_{t=1}^L P_\phi(x_t|x_{<t}, \mathbf{Z}). \quad (2)$$

**Training objective.** The training loss of compressor combines reconstruction fidelity and generative capability:

$$\begin{aligned} \mathcal{L} &= \mathcal{L}_{\text{re}} + \mathcal{L}_{\text{nt}} \\ &= - \sum_{t=1}^k \log P_\phi(x_t|x_{<t}, \mathbf{Z}) - \sum_{t=k+1}^n \log P_\phi(x_t|x_{<t}, \mathbf{Z}), \end{aligned} \quad (3)$$

here,  $\mathcal{L}_{\text{re}}$  enforces faithful reconstruction of the compressed prefix  $x_{1:k}$  conditioned on  $\mathbf{Z}$ , while  $\mathcal{L}_{\text{nt}}$  applies standard autoregressive prediction to the continuation  $x_{k+1:n}$ .

Unlike abstractive summarization which allows paraphrasing, our objective is exact reconstruction, any deviation from the verbatim input is treated as information loss.

## 4. The Size-Fidelity Paradox

In this section, we begin by characterizing **The Size-Fidelity Paradox** through two dissection tasks designed to isolate distinct failure modes. Specifically, we demonstrate that larger models exhibit a heightened propensity for *knowledge overwriting*, where source facts are substituted with internal knowledge, and *semantic drift*, in which loose restructuring is prioritized over verbatim preservation. These results confirm that fidelity loss is a systematic consequence of scaling rather than random error.

### 4.1. Model Selection & Scale Range

To enable a rigorous analysis of scaling behavior under context compression, we evaluate compressor models drawn from two widely used model families, Qwen-3 (Yang et al., 2025a) and LLaMA-3.2 (Grattafiori et al., 2024), spanning nearly three orders of magnitude in parameter count, from 0.6B to 90B. All models are trained on high-quality text chunks sampled from the Fineweb dataset (Penedo et al., 2024), using an identical training protocol to minimize confounding factors. Tab. 1 summarizes our dataset configuration for these experiments.

For each model size, we train compressors at three compression rates (4 $\times$ , 16 $\times$ , and 64 $\times$ ). Before turning to spe-

Task	Dataset	#Contexts	#QAs
Reconstruction	Fineweb	4,444,672	–
Knowledge Overwriting	FaithEval	598	598
	ConflictQA	1431	1431
Semantic Drift	Fineweb	449	8980
	FaithEval	598	11960

Table 1. Task and dataset statistics.

specific failure modes, we first examine the global training dynamics across scale. As shown in Fig. 2, larger models consistently exhibit more favorable optimization behavior. They descend more steeply and converge to the loss floor substantially faster than smaller models. Superficially, this pattern suggests that scaling improves learning efficiency under the compression objective. However, as we show in the following sections, this apparent success is misleading. Despite superior convergence and lower training loss, larger models increasingly fail to preserve the underlying input information, revealing a disconnect between optimization performance and reconstructive fidelity.

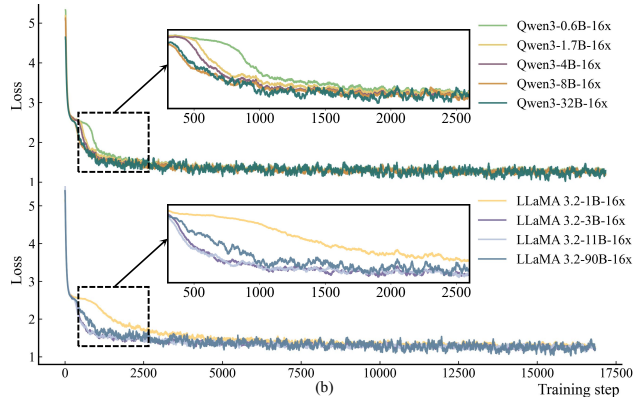


Figure 2. Training loss dynamics for Qwen (top) and LLaMA (bottom) compressors at a 4× compression rate. Larger models exhibit faster convergence and lower final loss, creating a deceptive signal of superior optimization.

## 4.2. Dissection1: Knowledge Overwriting

**Definition.** We define *knowledge overwriting* as the first failure mode in which a compression model prioritizes its parametric world knowledge over conflicting source context, generating outputs that deviate from the compressed input and exhibit reduced factual fidelity.

**Evaluation Setup.** To isolate and quantify this phenomenon, we design a controlled counterfactual evaluation. We curate a dataset from FaithEval (Ming et al., 2024) and Conflic-

tQA (Xie et al., 2024), both of which introduce deliberate factual contradictions into otherwise natural contexts (e.g., replacing “Einstein was born in Germany” with “Einstein was born in France”). We retain only samples in which the counterfactual modification is unambiguous and the corresponding real-world fact is well established, ensuring a clear and explicit conflict between the source evidence and the model’s parametric knowledge.

Each counterfactual context is first compressed by the target compressor model and then paired with a question that directly queries the modified fact. For each question, we provide two categories of candidate answers: **i**) the counterfactual answer consistent with the compressed context, and **ii**) alternative answers that are plausible under common world knowledge. We measure *knowledge faithfulness* as the accuracy of selecting the counterfactual answer, which reflects the model’s ability to prioritize compressed source information over its internal priors.

**Results and Analysis.** In Tab. 2, the knowledge overwriting QA section compares FaithEval (Ming et al., 2024) and ConflictQA (Xie et al., 2024) across Qwen3 and LLaMA-3.2 model scales. As model size increases, the two metrics decouple: while both improve from 0.6B to 4B parameters, further scaling leads to monotonically higher BLEU but sharply degraded faithfulness. Notably, under a 16× compression rate, the 90B model attains a much lower FaithEval faithfulness accuracy (0.55) than the 4B model (0.71), even though it achieves comparable reconstruction quality. This non-monotonic trend is consistent across model families, indicating a scale-driven effect whereby larger models increasingly override compressed counterfactual evidence with their parametric world knowledge.

## 4.3. Dissection2: Semantic Drift

**Definition.** We define *semantic drift* as the second failure mode in which a compression model maintains surface fluency and topical coherence while subtly distorting the underlying semantic or relational structure of the source. Unlike knowledge overwriting, semantic drift arises from structural degradation during paraphrastic compression rather than factual conflict.

**Evaluation Setup.** Existing benchmarks focus on topical relevance or factual recall and are largely insensitive to fine-grained structural distortions such as role reversal or modifier loss. To address this gap, we construct a diagnostic QA dataset over FineWeb (Penedo et al., 2024) and FaithEval (Ming et al., 2024) passages, using DeepSeek-R1 (Guo et al., 2025) to generate targeted questions that probe whether compression preserves precise semantic and relational structure rather than merely capturing topical gist.

Specifically, we evaluate seven dimensions along which

When Less is More: The LLM Scaling Paradox in Context Compression

Compression Rate	Model	#Params	Reconstr.	Knowledge Overwriting		Semantic Drift	
			Fineweb	FaithEval	ConflictQA	Fineweb	FaithEval
4×	Qwen 3	0.6b	0.95 (-0.02)	0.71 (-0.05)	0.95 (-0.02)	0.83 (-0.04)	<b>0.83</b>
		1.7b	0.94 (-0.03)	<b>0.76</b>	0.89 (-0.06)	0.83 (-0.04)	0.81 (-0.02)
		4b	0.94 (-0.03)	0.72 (-0.04)	<b>0.95</b>	<b>0.87</b>	0.79 (-0.0)
		8b	0.94 (-0.03)	0.74 (-0.02)	0.91 (-0.04)	0.79 (-0.04)	0.83 (-0.00)
	LLaMA 3.2	32b	<b>0.97</b>	0.68 (-0.08)	0.80 (-0.15)	0.60 (-0.27)	0.78 (-0.05)
		1b	0.94 (-0.03)	<b>0.77</b>	0.88 (-0.03)	0.78 (-0.01)	<b>0.85</b>
		3b	0.90 (-0.07)	0.74 (-0.03)	<b>0.91</b>	<b>0.79</b>	0.84 (-0.01)
		11b	0.92 (-0.05)	0.65 (-0.12)	0.80 (-0.11)	0.64 (-0.15)	0.76 (-0.09)
16×	Qwen 3	90b	<b>0.97</b>	0.60 (-0.17)	0.81 (-0.10)	0.59 (-0.20)	0.68 (-0.17)
		0.6b	0.83 (-0.03)	0.70 (-0.05)	0.94 (-0.00)	0.75 (-0.07)	0.84 (-0.02)
		1.7b	0.86 (-0.00)	<b>0.75</b>	0.88 (-0.06)	0.79 (-0.03)	<b>0.86</b>
		4b	<b>0.86</b>	0.71 (-0.04)	<b>0.94</b>	<b>0.82</b>	0.83 (-0.03)
	LLaMA 3.2	8b	0.84 (-0.02)	0.72 (-0.03)	0.89 (-0.05)	0.73 (-0.09)	0.79 (-0.07)
		32b	0.85 (-0.01)	0.61 (-0.14)	0.72 (-0.22)	0.57 (-0.25)	0.74 (-0.12)
		1b	0.82 (-0.04)	0.72 (-0.01)	0.84 (-0.06)	0.75 (-0.00)	0.90 (-0.00)
		3b	0.81 (-0.05)	<b>0.73</b>	<b>0.90</b>	<b>0.75</b>	<b>0.90</b>
64×	Qwen 3	11b	0.85 (-0.01)	0.63 (-0.10)	0.77 (-0.13)	0.61 (-0.14)	0.73 (-0.17)
		90b	<b>0.86</b>	0.55 (-0.18)	0.74 (-0.16)	0.56 (-0.19)	0.63 (-0.27)
		0.6b	0.17 (-0.12)	0.44 (-0.10)	0.59 (-0.11)	0.31 (-0.10)	0.39 (-0.20)
		1.7b	0.21 (-0.08)	0.51 (-0.03)	0.60 (-0.10)	0.35 (-0.06)	0.42 (-0.07)
	LLaMA 3.2	4b	0.27 (-0.02)	<b>0.54</b>	<b>0.70</b>	<b>0.41</b>	0.46 (-0.03)
		8b	0.28 (-0.01)	0.54 (-0.00)	0.67 (-0.03)	0.38 (-0.03)	<b>0.49</b>
		32b	<b>0.29</b>	0.47 (-0.07)	0.56 (-0.14)	0.27 (-0.14)	0.35 (-0.14)
		1b	0.19 (-0.14)	0.49 (-0.06)	0.57 (-0.11)	0.33 (-0.02)	0.44 (-0.03)

Table 2. Quantitative Evaluation of the Size-Fidelity Paradox across Llama and Qwen Families (0.6B–90B). We report reconstruction performance (BLEU) and QA accuracy for *Knowledge Overwriting* and *Semantic Drift* under varying compression rates across 3 datasets: Fineweb, FaithEval, and ConflictQA. **Bold** values indicate the best-performing model within each specific family, compression rate, and dataset, while **blue** and **gray** parentheses denote the performance delta relative to these top-performing models within the same group.

semantic drift frequently occurs: (1) *main topic*, testing whether the central subject or domain shifts; (2) *entity list*, detecting degradation of specific entities into coarse categories (e.g., “Nike and Adidas” → “sportswear brands”); (3) *predicate exactness*, assessing preservation of key verbs and relational predicates; (4) *relation anchor*, verifying maintenance of causal, contrastive, or conditional links across sentences; (5) *coreference*, checking correct resolution of pronouns to their antecedents; (6) *role binding*, ensuring accurate “who did what to whom” assignments; and (7) *modifier scope*, testing retention of qualifiers and constraints that prevent over-generalization.

To ensure high precision, all answerable questions require exact substring matches from the original context, eliminating ambiguity from paraphrased or pronoun-only responses. In addition, each context includes unanswerable-but-plausible questions to detect hallucinated details. This design yields a stringent diagnostic in which models must preserve structural and relational fidelity, rather than merely topical keywords.

**Results and Analysis.** Tab. 2 shows a non-monotonic relationship between structural QA accuracy and BLEU across model scales, closely mirroring the knowledge overwriting trend. Structural fidelity improves from 0.6B to 4B parameters as models gain capacity to handle complex syntax, but degrades beyond this point despite continued gains in BLEU. This divergence reflects a failure mode distinct from factual overwriting. Larger models increasingly capture semantic gist and generate fluent reconstructions, yet become less sensitive to fine-grained relational constraints, leading to systematic semantic drift. Overall, scaling appears to favor abstract semantic compression at the expense of precise structural preservation.

## 5. Paradox Analysis

Previous sections have shown that increasing model scale can degrade fidelity under context compression. To go beyond scale-level observations, we further probe the memory embeddings  $\mathbf{Z} \in \mathbb{R}^{m \times d}$  (defined in §3), which form

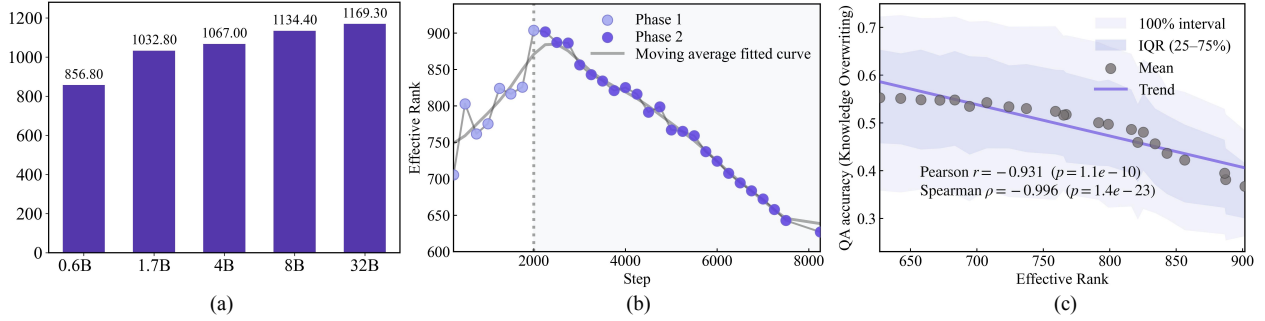


Figure 3. (a) Effective rank increases monotonically with model scale in the Qwen3 family (0.6B–32B). (b) **Training dynamics of effective rank.** A clear two-phase trajectory emerges: early expansion followed by compression. (c) **Effective rank vs. QA performance.** Effective rank is negatively correlated with QA accuracy; shaded bands indicate the sample-level distribution.

the sole interface between the compressor and the decoder. Specifically, we employ two complementary dimensions that characterize the behavior of  $\mathbf{Z}$  under scaling. The first is *semantic capacity*, which we measure using the effective rank of memory embeddings to probe the richness of its representation. The second is *generative uncertainty*, which we quantify using the conditional entropy of token predictions during reconstruction. Together, these dimensions characterize how information is represented in the compressed representation and how it is manifested during decoding.

### 5.1. Semantic Capacity Enables Knowledge Overwrite

**Scaling trends of effective rank.** Faithful compression favors representations that preserve source-specific information in compact form rather than dispersing it across a broad semantic space. As representations become more distributed, they admit greater semantic flexibility, increasing opportunities for parametric priors to interfere with source content. Formally, given the memory embeddings  $\mathbf{Z} \in \mathbb{R}^{M \times d}$  produced by the compressor, we flatten them across samples in a batch to obtain  $\mathbf{Z}_{\text{batch}} \in \mathbb{R}^{B \times D}$ , where  $D = M \times d$ . We compute the effective rank as the exponential of the spectral entropy over singular values:  $\text{erank}(\mathbf{Z}) = \exp(-\sum_{i=1}^r p_i \log p_i)$ , where  $p_i = \frac{\sigma_i}{\sum_{j=1}^r \sigma_j}$ , and  $\sigma_1 \geq \sigma_2 \geq \dots \geq \sigma_r$  denote the singular values of  $\mathbf{Z}$ .

Empirically, as illustrated in Fig. 3(a), we find that effective rank increases monotonically with model scale across the Qwen3 family (0.6B–32B), confirming that larger models produce more distributed representations—and thus face greater vulnerability to prior interference.

**Training Dynamics of Rank.** To further disentangle model size from the intrinsic role of semantic capacity, we fix the architecture and examine how effective rank evolves throughout the training process. The results are illustrated in Fig. 3(b), which tracks effective rank over 8,000 training

steps for Qwen3-0.6B under  $16\times$  compression.

We observe that the trajectory exhibits a striking non-monotonic pattern: rank rises sharply in early training, peaks around step 2,000, then declines steadily toward convergence – suggesting two distinct learning regimes. In the first phase, the model initialized to explores the representational landscape. As it learns vis diverse inputs, it expands the active subspace to differentiate samples and capture statistical regularities in the data. The subsequent *compression phase* aligns with the information bottleneck principle (Godey et al., 2024): after establishing a broad semantic scaffold, the model discards irrelevant dimensions, converging toward a lower-dimensional manifold that retains only essential structure for verbatim reproduction.

**Rank-Fidelity Correlation.** To verify whether high semantic capacity causally drives knowledge overwriting, we examine the relationship between rank and QA faithfulness of knowledge overwriting by leveraging the training dynamics described above. To avoid confounding the learning of basic capabilities with representational shifts (Simpson’s paradox (Wagner, 1982)), we restrict our analysis to the post-peak steps, where the model possesses established knowledge structures. We ask a more targeted question: *once the model has learned what to represent, does higher rank facilitate or hinder faithful reconstruction?*

We measure the correlation between effective rank and knowledge faithfulness across various effective ranks. Fig. 3(c) shows the results using quantile bands (IQR) to demonstrate stability. The mean trajectory exhibits a pronounced negative slope, and the tight quantile bands confirm this trend holds across individual samples rather than being driven by outliers. Moreover, we observe a robust linear correlation ( $r = -0.931, p = 1.1 \times 10^{-10}$ ) reinforced by a near-perfect monotonic relationship (Spearman  $\rho = -0.996, p = 1.4 \times 10^{-23}$ ). These metrics indicate

that within the compression regime, effective rank acts as a systematic predictor of faithfulness rather than a spurious correlate. Further, these findings identify semantic capacity as a mechanistic culprit behind Size-Fidelity Paradox: while larger models possess potential for richer representations, this very capacity prevents collapse into the low-rank manifold necessary for faithful verbatim reproduction.

## 5.2. Generative Uncertainty Drives Semantic Drift

**Scaling Trends of Conditional Entropy.** While effective rank characterizes the semantic capacity of the embedding space  $\mathbf{Z}$ , the phenomenon of conceptual drift manifests at generation time: even when the compressed content is semantically plausible, the decoder may choose among many locally fluent continuations that subtly alter relational structure. We quantify this generative uncertainty using the *conditional entropy* of the token prediction distribution.

Formally, given a compressed representation  $\mathbf{Z} = f_\theta(\mathbf{x})$ , the decoder defines an autoregressive distribution  $P_\phi(\mathbf{x} | \mathbf{Z}) = \prod_{t=1}^L P_\phi(\mathbf{x}_t | \mathbf{x}_{<t}, \mathbf{Z})$ , consistent with the reconstruction objective in Sec. 3. At each step  $t$ , we compute the Shannon entropy over the vocabulary:  $H_t(\mathbf{Z}) = -\sum_{v \in \mathcal{V}} P_\phi(v | \mathbf{x}_{<t}, \mathbf{Z}) \log P_\phi(v | \mathbf{x}_{<t}, \mathbf{Z})$ , and define the sample-level conditional entropy as the time average  $H(\mathbf{Z}) = \frac{1}{T} \sum_{t=1}^T H_t(\mathbf{Z})$ , where  $T$  is the number of evaluated reconstruction tokens. Specifically, we compute  $H(\mathbf{Z})$  under teacher forcing to remove variability from free-form decoding and isolate the decoder’s intrinsic uncertainty conditioned on  $\mathbf{Z}$ .

Fig. 4(a) presents the entropy distribution across varying model scales (0.6B to 90B). Strikingly, the trend is non-monotonic: entropy decreases from 0.6B to 4B, then rises from 4B to 90B across both Qwen and LLaMA families. This indicates a qualitative shift with scale. For smaller models (0.6B–4B), increasing scale improves the model’s ability to fit the data manifold, resulting in sharper, more confident predictions (lower entropy). Mid-sized compressors become more confident in token-level reconstruction, whereas larger compressors re-enter a higher-entropy regime where multiple paraphrastic continuations remain competitive.

**Training Dynamics of Entropy.** To identify the underlying mechanism driving semantic drift, we hypothesize that variations in generative uncertainty—rather than raw capacity—dictate performance. Here, we fix the model size and examine how entropy evolves during the training.

Fig. 4(b) tracks entropy for Qwen3-0.6B over 8,000 training steps at 16 $\times$  compression, measured every 750 steps. In contrast to the non-monotonic scaling trend, the temporal dynamic shows a consistent monotonic decrease. This trajectory indicates that the compressor progressively learns to sharpen the decoder’s distribution. As training proceeds, the

system transitions from an exploratory phase to a committed reconstruction strategy, reducing the ambiguity passed to the decoder. Critically, this training-induced entropy reduction provides a baseline: when larger models reverse this trend and produce higher entropy despite more training, it signals an emergent property of scale that directly impacts generation fidelity.

**Entropy-Fidelity Correlation.** To investigate the predictive relationship between generative uncertainty and task performance, we analyze the correlation between sample-level entropy and reconstruction fidelity. Specifically, we evaluate the reconstruction fidelity using a specialized Drifting QA task, where each sample is probed with 20 factual questions to detect subtle hallucinations.

Fig. 4(c) reveals a strong, statistically significant negative correlation between conditional entropy and QA accuracy (Pearson  $r = -0.823$ , Spearman  $\rho = -0.876$ ). Samples triggering high entropy, whereby the decoder faces a flat probability distribution among multiple candidates, consistently yield lower accuracy on the drifting benchmark. This confirms a causal mechanism for drift: when the compressor cannot resolve the ambiguity in  $\mathbf{Z}$  to a single sharp peak (low entropy), it reverts to probabilistic sampling among “plausible but distinct” alternatives. These findings identify heightened generative uncertainty as another mechanistic culprit behind the *Size-Fidelity Paradox*. While larger models possess stronger capabilities, their inherent tendency toward high-entropy states creates a “creativity trap.” Rather than adhering to the conservative copying required for compression, larger models favors fluent paraphrasing over the rigid structural preservation necessary to prevent drift.

## 6. Ablation Study

To ensure the Size-Fidelity Paradox is not an artifact of a specific decoder configuration, we examine the transferability of our findings across different decoder architectures and scales. In our main experiments, we utilized a fixed Meta-Llama-3-8B-Instruct decoder. In this section, we test to verify whether the fidelity degradation in larger compressors persists under different decoding conditions. We evaluate compressors (0.6B, 4B, and 8B) at a fixed 16 $\times$  compression rate. The results are summarized in Tab. 3.

We train compressors from the Qwen3 family (0.6B, 4B, 8B) at a 16 $\times$  compression rate and evaluate them with decoders of varying capacity: Qwen3-0.6B and Qwen3-4B. This cross-family transfer (LLaMA $\rightarrow$ Qwen) tests whether the paradox generalizes beyond architectural specifics, while the decoder size ablation tests whether smaller decoders expose or suppress the fidelity degradation we observe in larger models.

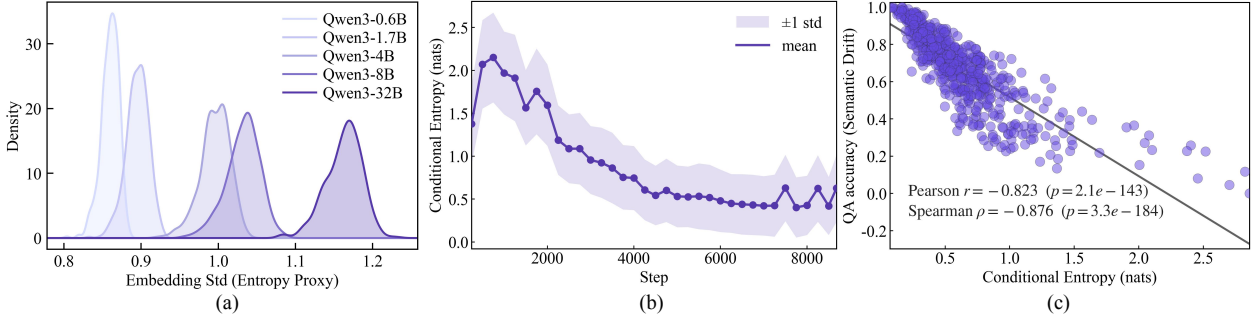


Figure 4. (a) Entropy distribution across model scales (0.6B–32B). (b) Training dynamics of conditional entropy (steadily decreasing over optimization). (c) Conditional entropy vs. QA accuracy (strong negative correlation: Pearson  $r = -0.823$ , Spearman  $\rho = -0.876$ ).

Compressor	Recons.		QA(i)		QA(ii)	
	Fineweb	FaithEval	ConflictQA	Fineweb	FaithEval	
<i>Decoder: Qwen3-0.6B      Compression Rate: 16x</i>						
Qwen3-0.6b	0.62	0.59	0.63	0.58	0.66	
Qwen3-4b	0.66	0.54	0.62	0.58	0.68	
Qwen3-8b	0.61	0.53	0.59	0.52	0.61	
<i>Decoder: Qwen3-4B      Compression Rate: 16x</i>						
Qwen3-0.6b	0.76	0.65	0.80	0.62	0.75	
Qwen3-4b	0.79	0.66	0.81	0.63	0.77	
Qwen3-8b	0.77	0.62	0.75	0.57	0.71	

Table 3. Ablation study on decoder generalizability. Quantitative evaluation of Qwen3 compressors (at 16 $\times$  compression) utilizing Qwen3-0.6B and Qwen3-4B as decoders. “Recons.” denotes reconstruction accuracy on FineWeb.

## 6.1. Results and Analysis

**Robustness to Decoder Scaling.** Tab. 3 presents reconstruction accuracy and QA performance across decoder configurations. When the decoder size is reduced from 8B to 4B, we observe a slight baseline drop in reconstruction metrics. However, the paradox remains pronounced: the 8B compressor continues to exhibit significantly higher rates of knowledge overwriting and semantic drift compared to the 4B compressor.

When using the 0.6B decoder, all compressors experience substantial degradation in both reconstruction and QA tasks, reflecting the decoder’s limited generation capacity. Crucially, this bottleneck narrows the performance gap between compressors—the 8B compressor’s tendency toward overwriting and drift is partially suppressed by the decoder’s constraints. However, the relative ordering persists: even under a weak decoder, the 8B compressor shows higher error rates on both QA tasks compared to the 0.6B and 4B compressors. This suggests that while decoder capacity

modulates the severity of the paradox, it does not eliminate the underlying mechanism.

**Universality Across Families.** Crucially, this experiment involves pairing Qwen-family compressors with Qwen-family decoders, whereas our main experiments used Llama-family decoders. The persistence of the paradox across this architectural transfer confirms that the fidelity loss is intrinsic to the scaled compressor’s representation space, rather than a compatibility artifact between specific model families.

**Universality Across Families.** Crucially, this experiment involves pairing Llama-family compressors with Qwen-family decoders. The persistence of the paradox in this cross-family setting confirms that the fidelity loss is intrinsic to the scaled compressor’s representation space, rather than a compatibility issue between specific model architectures.

## 7. Conclusion

This work has demonstrated that the prevailing intuition behind parameter scaling does not straightforwardly transfer to lossy context compression. Across experiments ranging from 0.6B to 90B model parameters, we have shown a Size-Fidelity Paradox: larger compressors achieve lower training loss yet produce less faithful compressed representations. To pinpoint how fidelity erodes, we have introduced two diagnostic QA tasks that separately measure knowledge overwriting and semantic drift, while isolating the effects of model scale. By holding parameter count fixed and probing the compressed representations, we have demonstrated that the culprit is not size but the semantic capacity and uncertainty that scale brings. These diagnostics reveal fidelity degradations that standard reconstruction evaluations overlook, establishing a principled guideline for assessing context compression effectiveness. More broadly, this work challenges the universality of scaling laws, highlighting domains where larger models may require fundamentally different design principles to achieve desired behaviors.

## Impact Statement

This paper presents work whose goal is to advance the field of Machine Learning, specifically context compression techniques for large language models. Our findings reveal fundamental limitations of scaling that could inform more efficient and faithful compression systems.

## References

- Achiam, J., Adler, S., Agarwal, S., Ahmad, L., Akkaya, I., Aleman, F. L., Almeida, D., Altenschmidt, J., Altman, S., Anadkat, S., et al. Gpt-4 technical report. *arXiv preprint arXiv:2303.08774*, 2023.
- Berton, G., Unnikrishnan, J., Tran, S., and Shah, M. Compllm: Compression for long context q&a. *arXiv preprint arXiv:2509.19228*, 2025.
- Cai, H., Li, Y., Yuan, R., Wang, W., Zhang, Z., Li, W., and Chua, T.-S. Exploring training and inference scaling laws in generative retrieval. In *Proceedings of the 48th International ACM SIGIR Conference on Research and Development in Information Retrieval*, pp. 1339–1349, 2025.
- Chen, D., Gao, F., Zhang, S., Zhuang, Y., Tang, S., Liu, Q., Wang, H., Yang, X., and Xu, M. Improving large models with small models: Lower costs and better performance. *Neural Networks*, pp. 108276, 2025.
- Dai, Y., Lian, J., Huang, Y., Zhang, W., Zhou, M., Wu, M., Xie, X., and Liao, H. Pretraining context compressor for large language models with embedding-based memory. In *Proceedings of the 63rd Annual Meeting of the Association for Computational Linguistics (Volume 1: Long Papers)*, pp. 28715–28732, 2025.
- Ge, T., Hu, J., Wang, L., Wang, X., Chen, S.-Q., and Wei, F. In-context autoencoder for context compression in a large language model. *arXiv preprint arXiv:2307.06945*, 2023.
- Godey, N., de la Clergerie, É., and Sagot, B. Why do small language models underperform? studying language model saturation via the softmax bottleneck. *arXiv preprint arXiv:2404.07647*, 2024.
- Grattafiori, A., Dubey, A., Jauhri, A., Pandey, A., Kadian, A., Al-Dahle, A., Letman, A., Mathur, A., Schelten, A., Vaughan, A., et al. The llama 3 herd of models. *arXiv preprint arXiv:2407.21783*, 2024.
- Guo, D., Yang, D., Zhang, H., Song, J., Zhang, R., Xu, R., Zhu, Q., Ma, S., Wang, P., Bi, X., et al. Deepseek-r1: Incentivizing reasoning capability in llms via reinforcement learning. *arXiv preprint arXiv:2501.12948*, 2025.
- Hoffmann, J., Borgeaud, S., Mensch, A., Buchatskaya, E., Cai, T., Rutherford, E., Casas, D. d. L., Hendricks, L. A., Welbl, J., Clark, A., et al. Training compute-optimal large language models. *arXiv preprint arXiv:2203.15556*, 2022.
- Kaplan, J., McCandlish, S., Henighan, T., Brown, T. B., Chess, B., Child, R., Gray, S., Radford, A., Wu, J., and Amodei, D. Scaling laws for neural language models. *arXiv preprint arXiv:2001.08361*, 2020.
- Lai, H., Liu, X., Gao, J., Cheng, J., Qi, Z., Xu, Y., Yao, S., Zhang, D., Du, J., Hou, Z., et al. A survey of post-training scaling in large language models. In *Proceedings of the 63rd Annual Meeting of the Association for Computational Linguistics (Volume 1: Long Papers)*, pp. 2771–2791, 2025.
- Li, C., Liu, X., Zhang, Z., Zhang, S., Liu, S., Ma, G., Lan, Y., and Shen, C. Upfront chain-of-thought: A cooperative framework for chain-of-thought compression. *arXiv preprint arXiv:2510.08647*, 2025a.
- Li, Y., Dong, B., Guerin, F., and Lin, C. Compressing context to enhance inference efficiency of large language models. In *Proceedings of the 2023 conference on empirical methods in natural language processing*, pp. 6342–6353, 2023.
- Li, Z., Liu, Y., Su, Y., and Collier, N. Prompt compression for large language models: A survey. In *Proceedings of the 2025 Conference of the Nations of the Americas Chapter of the Association for Computational Linguistics: Human Language Technologies (Volume 1: Long Papers)*, pp. 7182–7195, 2025b.
- Li, Z., Su, Y., and Collier, N. 500xcompressor: Generalized prompt compression for large language models. In *Proceedings of the 63rd Annual Meeting of the Association for Computational Linguistics (Volume 1: Long Papers)*, pp. 25081–25091, 2025c.
- Lin, C.-Y. Rouge: A package for automatic evaluation of summaries. In *Text summarization branches out*, pp. 74–81, 2004.
- Lin, X., Ghosh, A., Low, B. K. H., Shrivastava, A., and Mohan, V. Refrag: Rethinking rag based decoding. *arXiv preprint arXiv:2509.01092*, 2025.
- Long, Y., Wu, X., Zhang, Y., Wen, X., Zhou, Y., and Hong, S. Copy-paste to mitigate large language model hallucinations. *arXiv preprint arXiv:2510.00508*, 2025.
- Longpre, S., Perisetla, K., Chen, A., Ramesh, N., DuBois, C., and Singh, S. Entity-based knowledge conflicts in question answering. *arXiv preprint arXiv:2109.05052*, 2021.

- Minderer, M., Gritsenko, A., and Houlsby, N. Scaling open-vocabulary object detection. *Advances in Neural Information Processing Systems*, 36:72983–73007, 2023.
- Ming, Y., Purushwalkam, S., Pandit, S., Ke, Z., Nguyen, X.-P., Xiong, C., and Joty, S. Faitheval: Can your language model stay faithful to context, even if “the moon is made of marshmallows”. *arXiv preprint arXiv:2410.03727*, 2024.
- Papineni, K., Roukos, S., Ward, T., and Zhu, W.-J. Bleu: a method for automatic evaluation of machine translation. In *Proceedings of the 40th annual meeting of the Association for Computational Linguistics*, pp. 311–318, 2002.
- Penedo, G., Kydlíček, H., Lozhkov, A., Mitchell, M., Raffel, C. A., Von Werra, L., Wolf, T., et al. The fineweb datasets: Decanting the web for the finest text data at scale. *Advances in Neural Information Processing Systems*, 37:30811–30849, 2024.
- Ruan, Y., Maddison, C. J., and Hashimoto, T. B. Observational scaling laws and the predictability of language model performance. *Advances in Neural Information Processing Systems*, 37:15841–15892, 2024.
- Sengupta, A., Goel, Y., and Chakraborty, T. How to upscale neural networks with scaling law? a survey and practical guidelines. *arXiv preprint arXiv:2502.12051*, 2025.
- Team, K., Bai, Y., Bao, Y., Chen, G., Chen, J., Chen, N., Chen, R., Chen, Y., Chen, Y., Chen, Y., et al. Kimi k2: Open agentic intelligence. *arXiv preprint arXiv:2507.20534*, 2025.
- Wagner, C. H. Simpson’s paradox in real life. *The American Statistician*, 36(1):46–48, 1982.
- Wang, Y., Li, K., Li, X., Yu, J., He, Y., Chen, G., Pei, B., Zheng, R., Wang, Z., Shi, Y., et al. Internvideo2: Scaling foundation models for multimodal video understanding. In *European Conference on Computer Vision*, pp. 396–416. Springer, 2024.
- Wei, J., Kim, N., Tay, Y., and Le, Q. Inverse scaling can become u-shaped. In *Proceedings of the 2023 Conference on Empirical Methods in Natural Language Processing*, pp. 15580–15591, 2023.
- Xie, J., Zhang, K., Chen, J., Lou, R., and Su, Y. Adaptive chameleon or stubborn sloth: Revealing the behavior of large language models in knowledge conflicts. In *Proceedings of ICLR*, 2024.
- Yang, A., Li, A., Yang, B., Zhang, B., Hui, B., Zheng, B., Yu, B., Gao, C., Huang, C., and Lv, C. Qwen3 technical report. 2025a.
- Yang, W., Wei, Q., Ma, C., Tan, W., and Yan, B. Scaling laws for data-efficient visual transfer learning. In *Proceedings of the 33rd ACM International Conference on Multimedia*, pp. 2968–2976, 2025b.
- Yen, H., Gao, T., and Chen, D. Long-context language modeling with parallel context encoding. In *Proceedings of the 62nd Annual Meeting of the Association for Computational Linguistics (Volume 1: Long Papers)*, pp. 2588–2610, 2024.
- Zhang, B., Luo, L., Chen, Y., Nie, J., Liu, X., Guo, D., Zhao, Y., Li, S., Hao, Y., Yao, Y., et al. Wukong: Towards a scaling law for large-scale recommendation. *arXiv preprint arXiv:2403.02545*, 2024.
- Zhou, L., Schellaert, W., Martínez-Plumed, F., Moros-Daval, Y., Ferri, C., and Hernández-Orallo, J. Larger and more instructable language models become less reliable. *Nature*, 634(8032):61–68, 2024.